1. Overview

1.1 Problem Significance
The tandem cylinder arrangement is a prototype for interaction problems commonly encountered in airframe noise configurations. For example, the oleo and hoses on a landing gear are closely spaced, nearly cylindrical bodies. The most upstream parts experience a nearly unperturbed incoming flow, and noise is generated by the unsteady flow around these bluff bodies. Whether regular vortex shedding is observed is dependent on cross-sectional shapes and the proximity of the parts. The interaction of unsteady wakes with downstream components creates an additional and often dominant source of noise. The tandem cylinder arrangement can be used to test the capability of numerical methods to simulate these effects.

1.2 Configuration
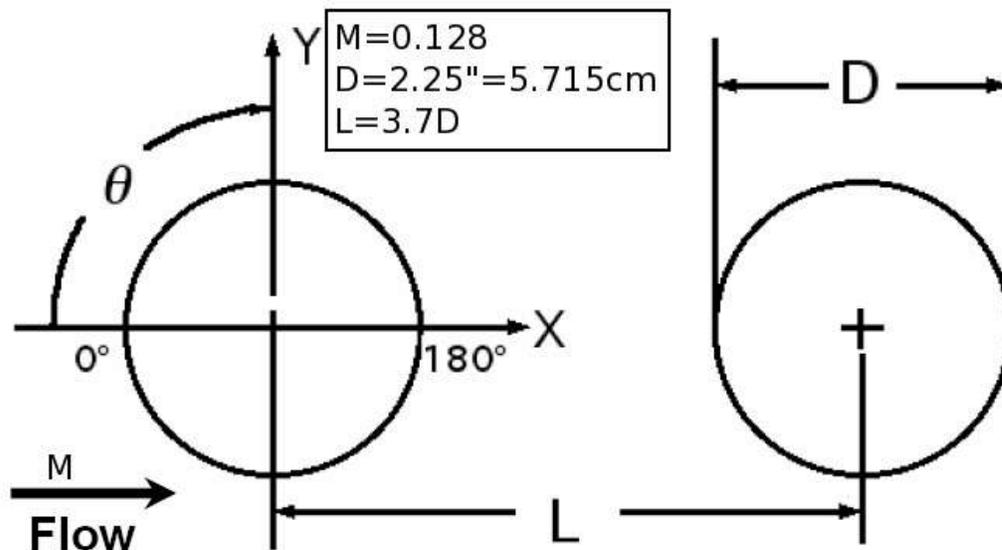
A series of experiments have been performed to collect data needed for such validation studies. A closed section wind-tunnel was used to obtain near-field aerodynamic data, and an open-jet, anechoic tunnel was used to both evaluate the sensitivity of the near-field data to the tunnel configuration and to measure the acoustic radiation. The flow Mach number selected for the workshop test case is 0.128 (corresponding to a reference velocity of U_o = 144 ft/s = 44 m/s at 70F (21C)) with identical cylinder diameters (D) of 2.25" (0.05715 m) resulting in a Reynolds number of 1.66×10^5. However, the experimental surface pressure results resemble those from tests with Reynolds numbers above 4 million, as a boundary layer trip was used on the upstream cylinder to insure a fully turbulent flow separation. Experimental results are available for cases with only the front cylinder tripped and with both cylinders tripped. Researchers should consider how they wish to simulate the important aspects of high Reynolds number flow.

For the selected separation distance of L = 3.7 D between the cylinder axes, the flow around the upstream cylinder is relatively unaffected by the downstream cylinder and experiences regular vortex shedding. Nonetheless, this challenges computational codes to properly simulate the turbulent boundary layer development, flow separation, and shear

layer roll-up. If the flow separates too early, the shear layers will spread too far apart and dramatically change the downstream wake. The surface pressure correlation in the spanwise direction doesn't go to zero until around 7 diameters, but three-dimensional effects are important and cannot be ignored. Ideally, calculations would employ a spanwise extent of similar order to that from the experiments. The span was 12.4 D in the closed-wind tunnel and 16 D in the open-jet tunnel. However, the computational cost for using a large spanwise extent can be prohibitive. Previous computations have shown that some of the important flow features can be captured with a span of 3 D. Therefore, the standard span length for the test case is $L_z = 3$ cylinder diameters with periodic boundary conditions, but researchers are strongly encouraged to use larger domains in addition to $L_z = 3D$. Scattering calculations [4] have identified some effects of the experimental arrangement on the radiated noise. Simulations that would further investigate the effect of the tunnel configuration are also encouraged.

With the flow dynamics from the upstream cylinder properly captured, calculations must then propagate the wake to the downstream cylinder and properly simulate the interaction with the solid surface. Although this interaction dominates the flow around the downstream cylinder, viscous boundary layer development is still important. Because the upstream cylinder experiences fairly regular vortex shedding, the interaction of these shed vortices with the downstream cylinder is also fairly regular. Hence, the surface pressure spectra and radiated noise exhibit strong spectral peaks at the primary shedding frequency, which is on the order of 200 Hz. There is a broadband component to the spectra, but it is at a much lower level. The acoustic directivity closely resembles the dipole shape observed for an isolated cylinder.

2. Problem Statement

Submissions are solicited for numerical simulations of the tandem cylinder arrangement. Both near-field aerodynamic data and information about the radiated acoustics is desired, but submissions with just the aerodynamic data will be accepted. Experimental data will be made available in the form of ascii text files. Tecplot™ layout files will be provided as well as figures showing the desired format for comparing simulation results with the experimental data in their papers. Participants will also submit their results to the organizers in the same format as the experimental data. The experimental data [1-4] that may be used for comparison with the simulations is outlined below.

Although the Mach number for the test case is 0.128, researchers may desire to run their simulations at larger Mach numbers to avoid numerical difficulties. Submissions will be accepted for Mach numbers up to 0.2, but the submitted data must be scaled to account for the differences in speed. All frequencies should be Strouhal scaled where $St = f D/U_o$, and the radiated noise should be assumed to follow $p'^2 \sim U_o^6 St^2$.

For simulations employing periodic boundary conditions in the spanwise direction, authors are encouraged to assume homogeneity and average their data in the spanwise direction.

2.1 Comparisons with experimental data

a. Mean Flow

1) On the surface of both cylinders, time-averaged mean coefficient of pressure, $C_p = <p>/(1/2 \ \rho|U_o|^2)$, versus the angle θ, measured clockwise from the upstream stagnation point (see figure). The reference velocity $U_o = M \ c_o = 144$ ft/s = 44 m/s.

2) Time-averaged mean streamwise velocity on a line connecting the centroids of the cylinders ($<u>/U_o$ versus x/D along y = 0)

b. Unsteady Nearfield

Unsteady surface pressure

1) On the surface of both cylinders, root-mean-square (RMS) of the coefficient of pressure versus θ

2) Power spectral density of the pressure (dB versus Hz) on the upstream cylinder at $\theta = 135$ deg

3) Power spectral density of the pressure (dB versus Hz) on the downstream cylinder at $\theta = 45$ deg

4) Spanwise correlation of pressure (R_{pp} versus span/D) on the upstream cylinder at $\theta = 135$ deg from the stagnation point

5) Spanwise correlation of pressure (R_{pp} versus span/D) on the downstream cylinder at $\theta = 135$ deg

6) Spanwise coherence of pressure (γ^2 versus span/D) on the upstream cylinder at $\theta = 135$ deg. Use the primary shedding frequency based on (2.1.b.2) above.

7) Spanwise coherence of pressure (γ^2 versus span/D) on the downstream cylinder at $\theta = 135$ deg. Use the primary shedding frequency.

c. Turbulent Kinetic Energy

1) Time-averaged, two-dimensional, turbulent kinetic energy (TKE) ($1/2 \ (<u' \ u'> + <v' \ v'>)/U_o^2$) at all grid points in the x-y plane

2) 2-D TKE along y=0

3) 2-D TKE along x=1.5D

4) 2-D TKE along x=4.45D (0.75D downstream of the centroid of the rear cylinder)

d. **Acoustics**

1) Power spectral density of the radiated noise (dB versus Hz) at three locations within the mid-span plane (specified coordinates measured relative to the centroid of the upstream cylinder):

(-8.33D, 27.815D), (9.11D, 32.49D), (26.55D, 27.815D).

Researchers may attempt to correct the predictions from calculations using a short span (e.g. L_z=3D) using the experimentally observed spanwise coherence length and techniques in the literature [7], but the uncorrected data should also be provided to the organizers.

2.2 Code to code comparisons

Additionally, the following data is requested to allow code to code comparisons:

1) Primary shedding frequency based on the peak of the spectrum in 2.1.b.2
2) Mean drag on both cylinders, averaged over a minimum duration of 25 periods of the primary shedding frequency
3) Power spectral density of the unsteady lift and drag coefficients (per unit span) on the cylinders
4) Acoustic directivity ($<p'^2>\cos\theta$ vs $<p'^2>\sin\theta$) at radii of 26.67 and 1000 diameters from a point (9.11D, -2.4D) from the centroid of the upstream cylinder.

2.3 Data targeted towards better understanding of noise sources

1) RMS of the coefficient of pressure at all grid points in the x-y plane

3.1 Time Resolution and Unsteady Data Collection

While resolution of frequencies up to 5 kHz is of interest, submitting parties should maintain at a minimum a frequency resolution of 1 kHz for the unsteady flow field. In addition, the collected time histories should be of sufficient duration to allow the construction of three independent time segments from which the pressure PSD curves can be computed with a bin width that is equal to or smaller than 20 Hz. The reported PSD should be formed by averaging over the realizations from the different time segments.

3.2 Transient Data

For highly interactive and complex flows, the transient flow is of significant duration and can easily be mistaken with the expected final well-established unsteady flow. Inclusion of this initial transient segment in both the sampled time records and the construction of the mean quantities irrevocably corrupts the computed results.

Submitting authors must ensure that upon the start of data sampling in their time-accurate simulations, initial transients have been eliminated. At a minimum, the flow should be allowed to traverse a distance of 50 cylinder diameters before sampling. This equates to 0.065 s of simulation time. Authors are encouraged to examine time histories of multiple quantities to determine when the flow has passed the transient phase.

3.3 Convergence Metrics

The convergence behavior of the simulated flow field should be clearly demonstrated by every submitting author. As a global indicator, the lift and drag time histories on each cylinder should be reported. Authors should also process the Cp rms on the cylinders and the streamwise velocity along y=0 using subsets of the collected data and report on the variation.Demonstration of grid convergence is highly desirable but in most instances difficult to achieve. In addition to the finest resolution possible, all authors are encouraged to run their simulations at other (coarser) resolutions and report on the sensitivity of the solution to the grid.

3.4 Other Metrics

All submissions should provide the total grid count (e.g. number of nodes, cells, etc.) as well as the cell size nearest to the cylinder surfaces. The time step size should be reported along with the total number of time steps in the simulation. Additional data regarding the computational resources that should be furnished by the authors are: a) the type and number of CPUs utilized, b) the type of data communication used, c) the time required to advance the solution over 1 time step d) the time required to advance the solution 1 second e) the per node and total memory required to run the code.

4.0 References

1. Jenkins, L., Khorrami, M., Choudhari, M., and McGinley, C., "Characterization of Unsteady Flow Structures Around Tandem Cylinders for Component Interaction Studies in Airframe Noise," AIAA-2005-2812, 2005.

2. Jenkins, L., Neuhart, D., McGinley, C., Choudhari, M., and Khorrami, M., "Measurements of Unsteady Wake Interference Between Tandem Cylinders," AIAA-2006-3202, 2006.

3. Lockard, D., Khorrami, M., Choudhari, M., Hutcheson, F., Brooks, T., and Stead, D., "Tandem Cylinder Noise Predictions," AIAA-2007-3450, 2007.

4. Neuhart, D., Jenkins, L., Choudhari, M. and Khorrami, M., "Measurements of the Flowfield Interaction Between Tandem Cylinders," AIAA-2009-3275, 2009.

5. Tinetti, A. and Dunn, M., "Acoustic Simulations of an Installed Tandem Cylinder Configuration," AIAA-2009-3158, 2009.

6. Khorrami, M., Choudhari, M., Lockard, D., Jenkins, L., and McGinley, C., "Unsteady Flowfield Around Tandem Cylinders as Prototype for Component Interaction in Airframe Noise," AIAA Journal, Vol. 45, No. 8, 2007, pp. 1930-1941.

7. Seo, J., Chang, K., and Moon, Y., "Aerodynamic Noise Prediction for Long-Span Bodies, AIAA-2006-2573, 2006.

8. Khorrami, M., Lockard, D., Choudhari, M., Jenkins, L., McGinley, C., and Neuhart, D., "Simulations of Bluff Body Flow Interaction for Noise Source Modeling," AIAA-2006-3203, 2006.

Note: Publications by NASA authors are freely available from http://ntrs.nasa.gov.